GA–A22634

ENERGY AND PARTICLE TRANSPORT IN THE RADIATIVE DIVERTOR PLASMAS OF DIII–D

by
A.W. LEONARD, S.L. ALLEN, N.H. BROOKS, T.E. EVANS,
M.E. FENSTERMACHER, D.N. HILL, R.C. ISLER, C.J. LASNIER,
M.A. MAHDAVI, R. MAINGI, R.A. MOYER, T.W. PETRIE,
G.D. PORTER, M.J. SCHAFFER, M.R. WADE, J.G. WATKINS,
W.P. WEST, D.G. WHYTE, and R.D. WOOD

JUNE 1997

GA–A22634

ENERGY AND PARTICLE TRANSPORT IN THE RADIATIVE DIVERTOR PLASMAS OF DIII–D

by

A.W. LEONARD, S.L. ALLEN,[†] N.H. BROOKS, T.E. EVANS, M.E. FENSTERMACHER,[†] D.N. HILL,[†] R.C. ISLER,[‡] C.J. LASNIER,[†] M.A. MAHDAVI, R. MAINGI,[‡] R.A. MOYER,[Δ] T.W. PETRIE, G.D. PORTER,[†] M.J. SCHAFFER, M.R. WADE,[‡] J.G. WATKINS,[◊] W.P. WEST, D.G. WHYTE,[Δ] and R.D. WOOD[†]

This is a preprint of a paper to be presented at the Twenty-Fourth European Conference on Controlled Fusion and Plasma Physics, June 9–14, 1997, Berchtesgaden, Germany, and to be published in the *Proceedings*.

[†]Lawrence Livermore National Laboratory
[‡]Oak Ridge National Laboratory
[Δ]University of California, San Diego
[◊]Sandia National Laboratories

Work supported by
the U.S. Department of Energy
under Contract Nos. DE-AC03-89ER51114,
W-7405-ENG-48, DE-AC05-96OR22464, DE-AC04-94AL85000
and Grant No. DE-FG03-95ER54294

GA PROJECT 3466
JUNE 1997

ENERGY AND PARTICLE TRANSPORT IN THE RADIATIVE DIVERTOR PLASMAS OF DIII–D*

A.W. Leonard, S.L. Allen,† N.H. Brooks, T.E. Evans, M.E. Fenstermacher,† D.N. Hill,† R.C. Isler,‡ C.J. Lasnier,† M.A. Mahdavi, R. Maingi,‡ R.A. Moyer,◊ T.W. Petrie, G.D. Porter,† M.J. Schaffer, M.R. Wade,‡ J.G. Watkins,Δ W.P. West, D.G. Whyte,◊ R.D. Wood†
General Atomics, P.O. Box 85608, San Diego, CA 92186-5608

It has been argued [1] that divertor energy transport dominated by parallel electron thermal conduction, or $q_{||} = -\kappa T_e^{5/2}\, dT_e/ds_{||}$, leads to severe localization of the intense radiating region and ultimately limits the fraction of energy flux that can be radiated before striking the divertor target. This is due to the strong $T_e^{5/2}$ dependence of electron heat conduction which results in very short spatial scales of the T_e gradient at high power densities and low temperatures where deuterium and impurities radiate most effectively. However, we have greatly exceeded this constraint on DIII–D with deuterium gas puffing which reduces the peak heat flux to the divertor plate a factor of 5 while distributing the divertor radiation over a long length as shown in Fig. 1. We find that electron thermal conduction cannot account for the measured distribution of divertor radiation and energy transport. However, plasma convection at the ion sound speed through much of the divertor is consistent with our observations.

The transport of energy parallel to the magnetic field in the scrape-off-layer (SOL) can be described by [2],

$$\frac{d}{ds}\left[-\kappa T_e^{5/2}\frac{dT_e}{ds} + nv_{||}\left\{\frac{5}{2}(T_i + T_e) + \frac{1}{2}m_i v_{||}^2 + I_o\right\}\right] = S_E \qquad (1)$$

where s is the parallel field line length, κ is the parallel electron thermal conductivity, T_e and T_i are the electron and ion temperatures respectively, n is the plasma density, m_i is the ion mass, $v_{||}$ is the plasma fluid velocity parallel to the magnetic field, I_o is the atomic ionization potential (13.6 eV for a deuterium atom) and S_E represents volume sources and sinks of energy such as radiation, ionization, neutral collisions and charge-exchange. In this formulation we have combined the electron and ion energy and disregarded ion viscosity and perpendicular diffusion of energy. The first term in the energy transport equation is electron thermal conduction. The second group of terms is convection and allows transport of energy without a temperature gradient. Here we have included the ionization potential of the plasma in the convective term because we do not experimentally determine the ionization distribution, an energy sink, nor do we determine the fraction of radiation and target plate heat flux that results from plasma recombination.

To compare our radiating divertor plasmas to the energy transport described in Eq. (1), we use a divertor equilibrium with a lower X–point, as shown in Fig. 2, which allows divertor Thomson

*Work supported by U.S. Department of Energy under Contracts DE-AC03-89ER51114, W-7405-ENG-48, DE-AC05-96OR22464, DE-AC04-94AL85000 and Grant No. DE-FG03-95ER54294.
†Lawrence Livermore National Laboratory.
‡Oak Ridge National Laboratory.
◊University of California, San Diego.
ΔSandia National Laboratories.

scattering diagnostic (DTS) [3,4] measurement of the divertor plasma electron temperature and density. Sweeping the divertor plasma across the DTS measurement locations, while holding plasma conditions constant, provides 2D profiles of temperature and density. We obtain divertor data from ELMing H–mode plasmas with a plasma current, of 1.4 MA and safety factor q_{95} of ~4.2 and injected power of about 6 MW. With strong deuterium puffing, ~100 Torr-ℓ/s, we produce intense divertor radiation, shown in Fig. 2, and reduce peak divertor plate heat flux by a factor of 3–5, or a factor of 5–10 if we subtract the contribution of radiative heating of the target plate [5].

The power flowing through the outboard divertor leg is described by $\nabla \bullet q_{||} = S_E$ where $q_{||}$ is the parallel heat flux, the sum of conduction and convection, and S_E, the plasma volume sources and sinks of energy, is due principally to atomic radiation. For this analysis we treat the SOL below the X–point as a 1D plasma as a function of $L_{||}$, the field line parallel distance to the divertor plate. The plasma radiation, ε ($L_{||}$), measured by two poloidally separated bolometer arrays [6], is integrated radially through the divertor SOL to produce a 1D profile of radiation, $\varepsilon_{sol}(z)$, as a function of distance from the divertor plate. We calculate the total energy flowing in the divertor, $Q_{tot}(z)$, by starting with the divertor target heat flux measured by an IR camera and integrating the 1D radiation profile. Contributions from plasma radiation are subtracted from the target heat flux. We finally convert to energy flux density, $q_{||}$ ($L_{||}$), by dividing by the cross-sectional area of the SOL perpendicular to the magnetic field. The SOL area normal to the magnetic field lines is determined by the heat flux width at the divertor plate in conjunction with magnetic equilibrium measurements. The parallel path length, $L_{||}$ is determined by mapping of a field line in the center of the SOL.

With no gas puffing we find the electron temperature profile to be consistent with conductive transport. The $q_{||}$ profile, shown in Fig. 3(a) indicates 40 MW/m^2 flows into the outboard divertor leg below X–point with only about ~15% of it radiated before striking the divertor plate. Assuming parallel electron thermal conduction and then integrating $q_{||} = -\kappa T_e^{5/2} dT_e/ds$ from Eq. (1) with T_e of 20 eV near the target we arrive at the conduction-fitted T_e profile as plotted in Fig. 3(a). We compare this fitted T_e profile with the T_e profile measured by DTS, averaged over the same SOL

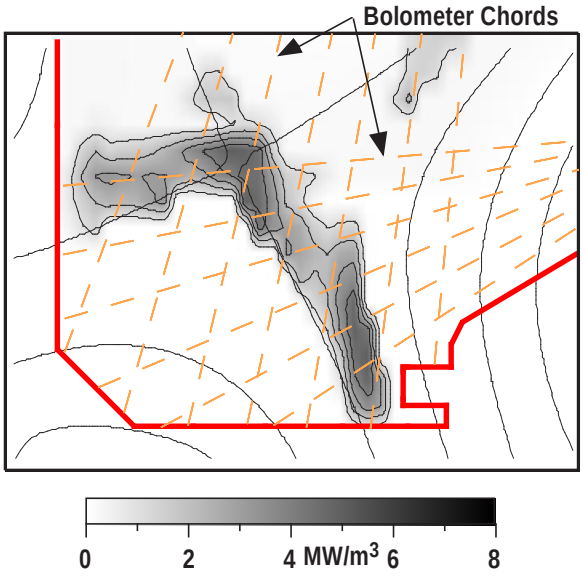

Fig. 1. The radiation profile for a radiative divertor in extended geometry in DIII–D.

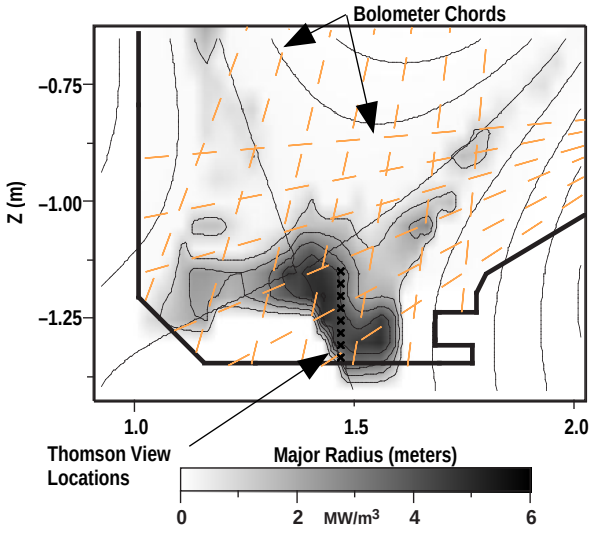

Fig. 2. The 2D radiation profile and divertor geometry for radiative plasmas used in heat transport analysis. Also shown are the bolomter view chords and the Divertor Thomson System measurement locations.

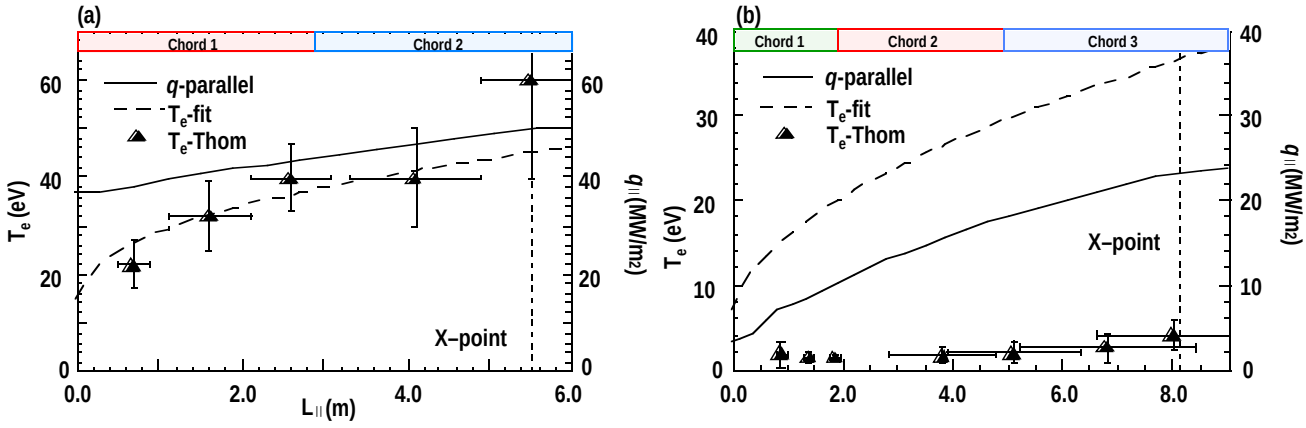

Fig. 3. The outboard divertor energy flux analysis for (a) standard ELMing H–mode and (b) radiative divertor through deuterium puffing. Shown are the energy flux profile, $q_{||}$, the fitted T_e profile for conduction dominated transport and measurements of T_e from divertor Thomson scattering measurements. Shown at the top of the graphs are the approximate view locations of the horizontal viewing bolometer chords.

width as that used in the $q_{||}$ calculation. The measured T_e, increasing from ~20 eV near the target to more than 40 eV at the X–point, is seen to be consistent with that inferred from conduction dominated energy transport.

Electron conduction cannot support the mesured energy flux in our highly radiating divertor plasmas. The energy transport in the divertor under these conditions is summarized in Fig. 3(b). Approximately 25 MW/m^2 of power flows into the divertor below the Xpoint, of which almost 85% is radiated away before reaching the divertor plate. The lower energy flux density into the divertor for the radiative case is due to a wider SOL width at the divertor plate for these plasmas and an increase in radiation above the Xpoint. The predicted T_e profile required to support the energy flux through conduction is also plotted in Fig. 2(b). Even for the modest energy flux at the divertor plate for these conditions T_e must rise above 15 eV in a relatively short parallel distance of ≤1 m, or ≤5 cm of poloidal length which is <15% of the total divertor length. The predicted T_e is in stark contrast to our DTS measurements where T_e is about 2 eV throughout the divertor. This level of T_e is able to support through conduction at most 5% of the energy flux we observe in these conditions.

Convection of plasma energy at the ion sound speed can account for our observed energy flux during these highly radiative conditions. Assuming the convection terms of Eq. (1) carry all of the energy flux we can solve for the required flow velocity using the measured profiles. The required Mach number, $c_s = \left[Zk\left(T_e + T_i\right)/m_i\right]^{1/2}$, is plotted in Fig. 4. The measured energy transport is satisfied if the plasma flows through the divertor at the ion acoustic speed before slowing as it nears the divertor target. Such an extended region of high plasma flow may follow as a consequence of T_e dropping to ~2 eV, so that the ionization mean free path is large enough (~30 cm) to shift the ionization far upstream near the X–point.

The observed radiation in the divertor is extracted from the plasma thermal energy, through electron excitation, and from the ionization potential through plasma recombination. To estimate the degree of plasma recombination we convert the inferred parallel plasma flow into particle flux, as plotted in Fig. 4. The uncertainty is large, but the data indicates that about half of the peak particle flux is lost, presumably through recombination, before reaching the divertor target.

Several other physical processes may also contribute to energy transport in the divertor, but their effects don't change the basic conslusions drawn above. In treating the SOL as 1D we have neglected

perpendicular diffusion which can widen the SOL from the X–point to the divertor. We have chosen the width of the SOL as that characteristic at the divertor plate. Because we have chosen the width of the SOL as that characteristic at the divertor plate any perpendicular diffusion may result in a more narrow upstream SOL than assumed in our analysis. This effect would lead to only a slightly greater T_e needed for conduction dominated transport due to the strong $T_e^{5/2}$ dependence of thermal conductivity. It is also possible for charge-exchange and ion-neutral collisions to carry away additional energy from the plasma. Neutrals likely contribute to our measured divertor target heat flux. Neutrals may also heat the divertor floor outside of the region of the SOL strike-point. This represents additional energy loss from the divertor plasma that we do not measure, which in turn may yield a greater $q_{||}$ upstream than our analysis indicates. The implications of this additional loss are the same as that of perpendicular diffusion we discussed above.

Edge-localized modes (ELMs) in these plasmas may play a role in the power balance of the divertor. The bursts of energy and particles due to ELMs may temporarily heat the SOL and divertor plasma allowing more power to be conducted for a short time. Analysis of ELMs on DIII–D [7] has shown that ≤10% of the injected power is dissipated in the outboard divertor during the brief ELM pulse, representing ≤20% of the total divertor power for these radiative plasmas. Though ELMs may play a role in the dynamic behavior of the divertor they do not account for the power flow observed in the experiment. Convection is still needed to explain our observed energy transport.

We have demonstrated nearly complete dissipation of of energy flowing into the DIII–D divertor. Convection allows high power levels to be transported through regions of cold plasma such that radiative cooling and finally recombination can occur through the divertor region. The convective flow is likely created by upstream ionization due to the low T_e and ionization rate in the divertor. More work is needed before these concepts can be applied to a high power density tokamak such as ITER. The plasma upstream of the convective zone must be cooled such that ionization, which produces the convection, can occur. Finally this must be implemented in such a way that confinement in the core plasma is not degraded.

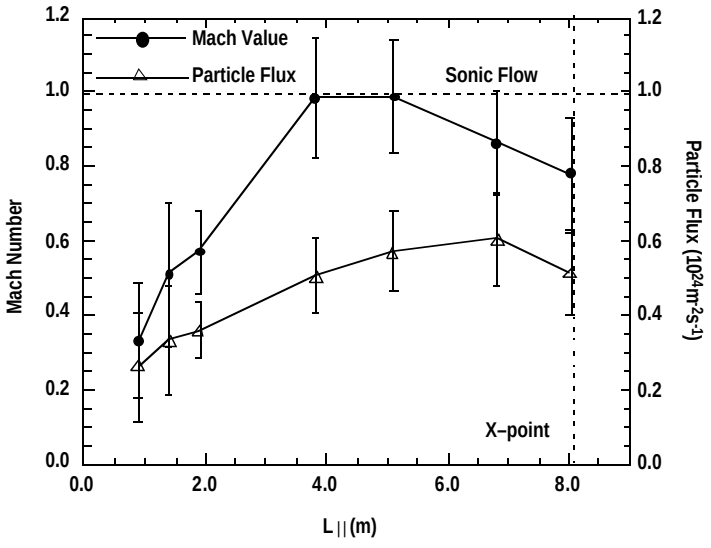

Fig. 4. The flow velocity, in Mach value, required to support the parallel energy flux through convection. Also plotted is the particle flux associated with the flow.

References

[1] K. Lackner, *et al.*, Fusion Engineering and Design **22** 107 (1993).

[2] S.I. Braginskii, "Transport Processes in a Plasma," in "Reviews of Plasma Physics," Vol 1 (M.A. Leontovich, Ed.) Consultants Bureau, New York 1965 p. 205.

[3] T.N. Carlstrom, *et al.*, Rev. Sci. Instrum. in print.

[4] S.L. Allen, *et al.*, J. Nucl. Mater., in print.

[5] T.W. Petrie, *et al.*, Nucl. Fusion **37** 321 (1997).

[6] A.W. Leonard, *et. al.*, Rev. Sci. Instrum. **66**, 1201 (1995).

[7] A.W. Leonard, *et al.*, J. Nucl. Mater., in print.